GEOPHYSICAL RESEARCH LETTERS, VOL. 26, NO. 23, PAGES 3465- 3468, DECEMBER 1, 1999

Diurnal cycle of rainfall and surface salinity in the western Pacific warm pool

Meghan F. Cronin and Michael J. McPhaden

Pacific Marine Environmental Laboratory, NOAA, Seattle, Washington

Abstract. The diurnal cycles of rainfall and surface salinity in the western equatorial Pacific were computed for the period August 1991–December 1994 using hourly data from the Tropical Atmosphere Ocean (TAO) mooring array enhanced for the Coupled Ocean Atmosphere Response Experiment (COARE). The analysis shows preferential rainfall during predawn hours. Nighttime mixing typically caused the predawn rainfall to mix downward into higher salinity subsurface waters. In contrast, afternoon rainfall, although weaker, generally produced a stable shallow layer of very low salinity. Consequently, sea surface salinity (SSS) exhibited a weak diurnal cycle, with anomalously low salinity in the late afternoon and anomalously high salinity at night. At 1 m depth, the SSS diurnal cycle anomalies were ∼0.005 psu. Although nearly two orders of magnitude less than the SSS standard deviation for this region, the anomalies were significant at the 95% confidence level.

Introduction

In the western equatorial Pacific warm pool, the sea surface temperature (SST) diurnal cycle has a dynamic range comparable to that of the intraseasonal to interannual variability. Consequently, there has been considerable research on whether the diurnal cycles observed in convection and rainfall are caused by the SST diurnal cycle [e.g., *Chen and Houze,* 1996]. In this analysis, we take the logical next step and ask whether the diurnal cycle in rainfall causes a diurnal cycle in sea surface salinity.

Buoy Array and Instrumentation

We use hourly Tropical Atmosphere Ocean (TAO) mooring data from the period August 1991–December 1994 (see Table1). During this period the TAO array was enhanced as a part of the Coupled Ocean Atmosphere Response Experiment (COARE)[*Webster and Lukas*, 1992]. Figure 1 shows the sites used in this study superimposed upon a map of the mean SST. Note that all sites lie within the convective region of the western Pacific warm pool.

Standard measurements on all TAO moorings include hourly wind speed and direction, air temperature, relative humidity, and SST[*McPhaden et al.*, 1998]. In addition, as a part of COARE, hourly rainrates were measured at six sites (2°N 156°E, 2°S 156°E, 0° 156°E, 0° 157.5°E, and 0° 165°E) using Science Technology model 105 optical rain gauges (ORGs). ORGs estimate rainrates based on scintillations of raindrops falling through a near-infrared light. Factory calibrations are the largest source of error for ORG rainrates, and are typically 25%, with occasionally larger errors[*Cronin and McPhaden*, 1998].

Hourly SSS and SST were measured at six sites (2°N 156°E, 2°S 156°E, 0° 156°E, 0° 160.5°E, and 0° 165°E) using Seabird SEACAT temperature and conductivity sensors mounted either on the toroid bridle 1 m below the surface, or on the mooring wire at 3 m depth. Additionally, some sites were instrumented with SEACATs at 5 m. When temperature and salinity were measured at both 1 m and 5 m (e.g., at 0° 156°E from September 1992 through April 1994), values were interpolated to 3 m. Likewise, for these periods, a 3 m vertical gradient was estimated by dividing the difference between the 1 m and 5 m time series by 4 m. SEACAT salinity errors are ∼0.02 psu and temperature errors are 0.005°C[*Cronin and McPhaden*, 1998; *Freitag et al.*, 1999].

Two buoys (0° 156°E and 0° 165°E) also measured hourly shortwave radiation with Eppley PSP radiometers. Thus, at these two sites, the net surface heat flux, Q_0, could be estimated by using the COARE version 2.5b bulk algorithm [*Fairall et al.*, 1996a, b] to estimate the latent and sensible heat fluxes and the *Clark et al.* [1974] bulk algorithm to estimate the net longwave radiation [e.g., *Cronin and McPhaden*, 1997].

Diurnal Cycle of Time Series

To compute the hourly composite time series of each variable, for each hour, all sites were averaged together and the time axis was converted from GMT to LST. Since 0° 165°E lies in the +11 hour time zone, while all other sites lie in the +10 hour time zone, prior to composite averaging, the 0° 165°E time series was shifted by 1 hour.

As shown in Figure 2, the hourly 1 m SSS time series has a standard deviation of ∼0.3 psu. Episodes of abrupt freshening in the hourly SSS time series are related to rainfall events. However, in the absence of other processes, rainfall would produce step-like features in the SSS time series, rather than spikes which so clearly characterize the SSS records. The rapid increase in SSS following the rainfall freshening is due to other processes such as mixing and advection which cause the surface salinity to rapidly increase following the rainfall freshening.

To distinguish the diurnal SST and SSS variability from lower frequency variability, "daily-highpassed" composite SST and SSS time series were computed by subtracting the 3-day triangular filtered composite time series from the hourly composite time series. The anomaly composite time series were then smoothed with a 1-2-1 filter, and binned according to hour to compute the diurnal cycle of the SST and SSS anomalies. Diurnal cycles of net surface heat flux, rainfall, and vertical temperature and salinity gradients were computed in a similar way but using the full, rather than the anomalous, composite time series. Because in all cases the integral timescale was less than one day, each day was con-

Copyright 1999 by the American Geophysical Union.

Paper number 1999GL9010504.
00948276/99/199GL9010504$05.00

Table 1. Start and End Dates for Precipitation (P), Net Surface Heat Flux (Q_0), and SEACAT Surface Temperature and Salinity Time Series Used in the Analysis

Site	P	Q_0	1 m SEACAT	3 m SEACAT	5 m SEACAT
0° 154°E	Nov 92–Aug 93	N/A	N/A	May 92–Mar 93	May 92–Mar 93
0° 156°E	Mar 92–Dec 94	Sep 92–Apr 94	Mar 92–Apr 94	Aug 91–Mar 92	Sep 92–Apr 94
0° 157.5°E	Sep 92–Jul 93	N/A	N/A	N/A	N/A
0° 160.5°E	N/A	N/A	N/A	May 92–Apr 94	May 92–Apr 94
0° 165°E	Feb 92–Dec 94	Aug 92–Dec 93	Feb 92–Apr 94	Aug 91–Feb 92	N/A
2°N 156°E	Sep 92–Dec 94	N/A	N/A	Sep 92–Feb 93	Sep 92–Feb 93
2°S 156°E	Sep 92–Dec 94	N/A	Sep 92–Feb 93	Sep 92–Apr 94	Sep 92–Feb 94

sidered statistically independent when computing the uncertainty of the mean diurnal cycle at the 95% confidence level.

Consistent with other studies [e.g., *Janowiak et al.,* 1994], the composite precipitation time series shows preferential rainfall during predawn hours (0300–0600 LST) (Figure 3). However, surprisingly, instead of inducing fresh SSS anomalies, the relatively heavy rainfall is associated with salty SSS anomalies. Maximum SSS anomalies occurred at 0500 LST, approximately in phase with the peak rainfall. Minimum SSS anomalies occurred in the late afternoon at 1800 LST. Although the SSS anomaly range (0.01 psu at 1 m and 0.004 psu at 3 m) is less than the accuracy of an individual SEACAT sensor, considerable averaging has gone into the ensemble and the values are significant at the 95% confidence level.

In order to analyze the rainfall and sea surface salinity diurnal cycles in relation to the thermal diurnal cycle, the net surface heat flux, Q_0, and precipitation, P, were each scaled to be buoyancy fluxes by assuming a linear equation of state (i.e., $B_Q = -g\alpha_T/(\rho c_p)\, Q_0$ and $B_P = -g\beta_S$SSS P, where g is gravity, α_T is the thermal expansion coefficient, β_S is the haline contraction coefficient, and ρc_p is the heat capacity per unit volume of the surface layer). Likewise, SST and SSS anomalies (dSST and dSSS) were scaled into buoyancy units according to $b_T = g\alpha_T\, d$SST and $b_S = -g\beta_S\, d$SSS.

As shown in Figure 3, during daytime, both the thermal buoyancy flux (B_Q) and haline buoyancy flux (B_P) tend to stabilize the water column. At night, though, B_Q is a destabilizing flux, while B_P is a stabilizing flux. Since the nighttime B_Q is nearly a factor of 2–3 larger than B_P, the water column destabilizes and nighttime mixing is expected during the strong predawn rainfall. Consequently, nighttime rainfall tends to be balanced by mixing and does not produce anomalous surface salinity freshening. In contrast, during the daytime, the net buoyancy flux tends to stabilize the ocean surface layer. Daytime mixing is reduced and afternoon rainfall, although relatively weak, is sufficient to produce the freshwater stratification and fresh surface salinity anomalies.

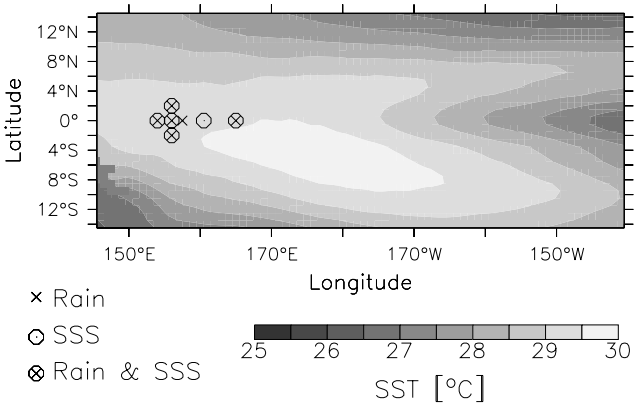

Figure 1. Buoy sites used in the analysis, superimposed upon the mean sea surface temperature for the period August 1991 through December 1994. Buoys with rain data are designated by an "x"; buoys with sea surface salinity (SSS) are designated by a circle; buoys with both SSS and rain are designated by an "x" within a circle.

Discussion

In the western Pacific warm pool, precipitation dominates over evaporation. Thus, assuming advection does not have a diurnal cycle, the diurnal cycle of SSS is controlled primarily by the diurnal cycles of precipitation and vertical mixing. The diurnal cycle of rainfall was computed using approximately 3 years of in situ rain data from six mooring sites in the western Pacific warm pool. In contrast, *Janowiak et al.* [1994] used 3 months of data from five of the mooring sites. However, the Janowiak et al. results were essentially unchanged. Although precipitation had substantial variability, accumulations were largest during the predawn hours of 0300–0600 LST.

Nevertheless, the buoyancy flux due to the surface heat flux dominated over the buoyancy flux due to rainfall. Consequently, the net surface buoyancy flux tended to destabilize the water column at night and generate nighttime turbulent mixing. Microstructure analyses[*Wijesekera and Gregg*, 1996] have shown that turbulent mixing has a pronounced diurnal cycle in this region, and that nighttime mixing and daytime warming can cause the mixed layer to deepen to ~20 m at night, and to shoal to within several meters of the surface during calm sunny days. Our analysis shows that this diurnal cycle of mixing has a profound effect on the diurnal cycle of SSS. Predawn rainfall tended to be quickly mixed downward and dissipated due to nighttime mixing, while afternoon rainfall produced a stable shallow fresh layer due to reduced daytime mixing. Thus, the combination of the diurnal cycles of mixing and rainfall resulted in surface salinity that was anomalously high in the early morning (0300–0700 LST) and anomalously low in the late afternoon (1400–2000 LST).

Understanding the diurnal cycle of rainfall and SSS is a particularly important issue for satellite measurements of these fields[*Lagerloef et al.*, 1995]. Typically, polar orbiting satellites do not resolve the diurnal cycle and aliasing can lead to significant biases [e.g., *Waliser and Zhou*, 1998]. Although there have been several case studies describing SSS variability over the course of a day [e.g., *Wijesekera and Gregg,* 1996], to the best of the authors' knowledge, this study represents the first open ocean SSS diurnal cy-

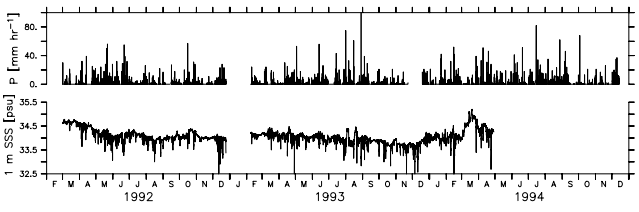

Figure 2. Hourly precipitation and 1 m SSS time series at 0° 156°E.

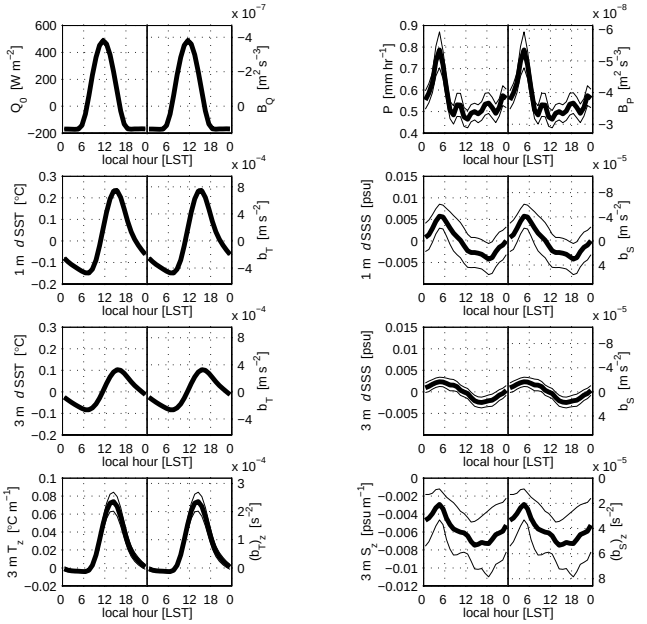

Figure 3. (Left column, thick lines) Diurnal cycles of the net surface heat flux, 1 m and 3 m SST anomaly, and 3 m vertical temperature gradient composites. (Right column, thick lines) Diurnal cycles of precipitation, 1 m and 3 m SSS anomaly, and 3 m vertical salinity gradient composites. The thin lines are the 95% confidence limits. The right axes show the corresponding buoyancy fluxes and surface buoyancies.

cle analysis ever performed. While there appears to be a statistically significant salinity diurnal cycle in the western equatorial Pacific, the salinity anomaly associated with the diurnal cycle is ∼0.005 psu at 1 m, nearly two orders of magnitude less than the SSS standard deviation, and certainly within the noise level of most salinity monitoring systems.

Acknowledgments. The authors thank R. Lukas (UH) for providing the 0° 154°E, 0° 160.5°E and 2°N 156°E SEACAT data, and the TAO Project Office for their work in maintaining the TAO array. This research was supported by NOAA's Office of Global Programs. This is PMEL contribution number 2009.

References

Chen, S. S., and R. A. Houze, Jr., Diurnal variations and life-cycle of deep convective systems over the tropical Pacific warm pool, *Q. J. R. Meteorol. Soc., 123,* 357–388, 1997.

Clark, N. E., L. Eber, R. M. Laurs, J. A. Renner, and J. F. T. Saur, Heat exchange between ocean and atmosphere in the eastern North Pacific for 1961–71, *NOAA Tech. Rep. NMFS SSRF-682,* U.S. Dep. Commer., Washington DC, 1974.

Cronin, M. F., and M. J. McPhaden, The upper ocean heat balance in the western equatorial Pacific warm pool during September–December 1992, *J. Geophys. Res., 102,* 8533–8553, 1997.

Cronin, M. F., and M. J. McPhaden, Upper ocean salinity balance in the western equatorial Pacific, *J. Geophys. Res., 103,* 27,567–27,587, 1998.

Fairall, C., E. F. Bradley, J. S. Godfrey, G. A. Wick, J. B. Edson, and G. S. Young, Cool skin and warm layer effects on sea surface temperature, *J. Geophys. Res., 101,* 1295–1308, 1996a.

Fairall, C., E. F. Bradley, D. P. Rogers, J. B. Edson, and G. S. Young, Bulk parameterization of air-sea fluxes for Tropical Ocean-Global Atmosphere Coupled-Ocean Atmosphere Response Experiment algorithm, *J. Geophys. Res., 101,* 3747–3764, 1996b.

Freitag, H. P., M. McCarty, C. Nosse, R. Lukas, M. J. McPhaden, and M. F. Cronin, COARE SEACAT data: Calibration and quality control procedures, *NOAA Tech. Memo. ERL PMEL-115,* Seattle, Wash., 89 pp., 1999.

Janowiak, J. E., P. A. Arkin, and M. Morrissey, An examination of the diurnal cycle in oceanic tropical rainfall using satellite and in situ data, *Mon. Wea. Rev., 122,* 2296–2311, 1994.

Lagerloef, G. S. E., C. T. Swift, and D. M. Le Vine, Sea surface salinity: The next remote sensing challenge, *Oceanography, 8,* 44–40, 1995.

McPhaden, M. J., et al., The Tropical Ocean Global Atmosphere (TOGA) observing system: A decade of progress, *J. Geophys. Res., 103,* 14,169–14,240, 1998.

Waliser, D. E., and W. Zhou, Removing satellite equatorial crossing time biases from the OLR and HRC datasets, *J. Clim., 10,* 2125–2146, 1998.

Webster, P. J., and R. Lukas, TOGA COARE: The Coupled Ocean-Atmosphere Response Experiment, *Bull. Am. Meteorol. Soc., 73,* 1377–1416, 1992.

Wijesekera, H. W., and M. C. Gregg, Surface layer response to weak winds, westerly bursts, and rain squalls in the western Pacific Warm Pool, *J. Geophys. Res., 101,* 977–997, 1996.

M. F. Cronin and M. J. McPhaden, Pacific Marine Environmental Laboratory, NOAA, 7600 Sand Point Way NE, Seattle, WA 98115 (cronin@pmel.noaa.gov; mcphaden@pmel.noaa.gov)

(Received June 07, 1999; accepted July 31, 1999.)